High-throughput glycopeptide profiling of prostate-specific antigen from seminal plasma by MALDI-MS

Wang, W.; Kaluza, A.; Nouta, J.; Nicolardi, S.; Ferens-Sieczkowska, M.; Wuhrer, M.; ... ; Haan, N. de

Talanta 222 (2021) 121495

Contents lists available at ScienceDirect

Talanta

journal homepage: www.elsevier.com/locate/talanta

High-throughput glycopeptide profiling of prostate-specific antigen from seminal plasma by MALDI-MS

Wei Wang [a,1], Anna Kałuża [b,1], Jan Nouta [a], Simone Nicolardi [a], Mirosława Ferens-Sieczkowska [b], Manfred Wuhrer [a], Guinevere S.M. Lageveen-Kammeijer [a,*,1], Noortje de Haan [a,*,1]

[a] Leiden University Medical Center, Center for Proteomics and Metabolomics, 2300, RC, Leiden, the Netherlands
[b] Wrocław Medical University, Department of Chemistry and Immunochemistry, Curie-Skłodowska Str. 50, 50-369, Wrocław, Poland

ARTICLE INFO

Keywords:
Prostate-specific antigen
Glycosylation
Sialic acids
Mass spectrometry
Infertility
Seminal plasma

ABSTRACT

An altered total seminal plasma glycosylation has been associated with male infertility, and the highly abundant seminal plasma glycoprotein prostate-specific antigen (PSA) plays an important role in fertilization. However, the exact role of PSA glycosylation in male fertility is not clear. To understand the involvement of PSA glycosylation in the fertilization process, analytical methods are required to study the glycosylation of PSA from seminal plasma with a high glycoform resolution and in a protein-specific manner. In this study, we developed a novel, high-throughput PSA glycopeptide workflow, based on matrix-assisted laser desorption/ionization-mass spectrometry, allowing the discrimination of sialic acid linkage isomers via the derivatization of glycopeptides. The method was successfully applied on a cohort consisting of seminal plasma from infertile and fertile men (N = 102). Forty-four glycopeptides were quantified in all samples, showing mainly complex-type glycans with high levels of fucosylation and sialylation. In addition, *N*,*N*-diacetyllactosamine (LacdiNAc) motives were found as well as hybrid-type and high mannose-type structures. Our method showed a high intra- and interday repeatability and revealed no difference in PSA glycosylation between fertile and infertile men. Next to seminal plasma, the method is also expected to be of use for studying PSA glycopeptides derived from other biofluids and/or in other disease contexts.

1. Introduction

Glycosylation is a highly complex post-translational modification that influences protein folding, solubility and protein-protein interactions [1]. Recently, associations were found between total seminal plasma (SP) glycosylation and an impaired fertility in men [2–4]. For example, α2,6-linked sialylation was found to be positively associated with sperm motility, while low α2,3-linked sialylation was associated with a reduced sperm count [3]. Furthermore, an increased fucosylation (α1,6-linked to *N*-acetylglucosamine or α1,3-linked to *N*-acetyllactosamine) was associated with infertility [4]. The higher degree of fucosylation was attributed to, amongst others, the glycoprotein prostate-specific antigen (PSA) [4]. This glycoprotein is highly abundant in SP, where it plays an essential role in increasing sperm motility by liquefying coagulated semen [5,6]. Furthermore, the elevated presence of PSA in male blood plasma is an important biomarker for the diagnosis of prostate cancer [7], making the analysis of this glycoprotein in different body fluids of high interest.

PSA contains one conserved *N*-linked glycosylation site at Asn_{69} [8,9] and an additional site was reported for the naturally occurring polymorphism $D_{102}\rightarrow N_{102}$ of the KLK3 gene [10]. In healthy individuals, PSA from SP carries mainly sialylated, diantennary complex-type glycans with a high degree of core fucosylation (α1,6-linked) and both LacNAc (galactose-β1,4-*N*-acetylglucosamine) and LacdiNAc

Abbreviations: PSA, prostate-specific antigen; SA, sialic acid; N, normozoospermic; A, asthenozoospermic; OA, oligoasthenozoospermic; O, oligozoospermic; C, control group; EEA, ethyl esterification of α2,6-linked SAs in combination with ammonia amidation of α2,3-linked SAs; DA, dimethylamine amidation of α2,6-linked SAs in combination with ammonia amidation of α2,3-linked SAs; LacdiNAc, *N*,*N*-diacetyllactosamine; SP, seminal plasma; bVHH-aPSA, biotinylated VHH *anti*-PSA antibodies; FA, formic acid; EDC, 1-ethyl-3-(3-(dimethylamino)propyl)-carbodiimide hydrochloride; HOBt, 1-hydroxybenzotriazole hydrate; ABC, ammonium bicarbonate.

* Corresponding author. University of Copenhagen, Copenhagen Center for Glycomics, 2200, Copenhagen N, Denmark.
E-mail addresses: g.s.m.kammeijer@lumc.nl (G.S.M. Lageveen-Kammeijer), ndehaan@sund.ku.dk (N. de Haan).
[1] Authors contributed equally.

https://doi.org/10.1016/j.talanta.2020.121495
Received 29 April 2020; Received in revised form 27 July 2020; Accepted 30 July 2020
Available online 13 August 2020

(*N*-acetylgalactosamine-β1,4-*N*-acetylglucosamine) motives on the antennae [11,12]. Furthermore, the presence of high mannose- and hybrid-type *N*-glycans as well as multiantennary complex-type structures and low degrees of sulfation have been reported [13–15].

Mass spectrometry (MS) is a core technology in the field of glycopeptide-based glycosylation profiling, however, identification and accurate quantification of isomeric glycoforms remains a challenging task. For the separation of sialic acid (SA) linkage isomers (α2,3- or α2,6-linked to the subterminal monosaccharide) on PSA, a high-performance PSA glycomics assay based on capillary electrophoresis (CE)-electro spray ionization (ESI)-MS was described recently [15]. Alternative separation techniques for SA isomers include reversed-phase liquid chromatography (LC) and porous graphitized carbon LC, optionally in combination with exoglycosidase treatment [16,17]. While these techniques provide high SA isomer resolution and high sensitivity (especially in the case of CE-ESI-MS), they are limited in throughput and ease of use. An attractive alternative for glycopeptide profiling is matrix-assisted laser desorption/ionization (MALDI)-MS, offering an accessible and high-throughput platform. However, the analysis of sialylated glycoconjugates by MALDI-MS is challenged by a biased ionization and salt adduct formation. Moreover, MS on itself is unable to differentiate between SA linkage isomers.

Recent efforts in optimizing derivatization strategies for both released glycans and glycopeptides have successfully addressed the challenges posed for MALDI-MS of sialylated analytes. At the released glycan level, SAs were differentially stabilized by ethyl or methyl esterification of the α2,6-linked SAs, while the α2,3-linked SAs lactonized, resulting in different masses for the isomeric species [18,19]. In addition, selective amidation strategies have been developed, which resulted in an increased stability of the α2,3-linked SAs. Similar methods have been applied for the derivatization of sialylated glycopeptides [20,21]. However, as of yet, no generally applicable protocol has been established for this purpose, mainly because the wide variety of different peptide portions result in different byproducts during the SA derivatization [20–22].

Here, a novel high-throughput protocol was developed for the characterization of SP PSA derived glycopeptides by MALDI-MS (Fig. 1). The workflow includes a bead-based affinity purification of PSA from SP, followed by reduction, alkylation and proteolytic digestion with trypsin. The PSA glycopeptides are subjected to a two-step amidation reaction (3 h total), which allows for stabilization and differentiation between α2,6- and α2,3-sialylated isomers [23]. All sample preparation steps can be performed in 96-well plate format and the final derivatization protocol results in minimal byproduct formation on the peptide portion.

The applicability and robustness of the developed assay was demonstrated in an intra- and interday repeatability assessment as well as by characterizing the SP PSA glycosylation profiles of men in a clinical setting (N = 102). The sample set consisted of fertile as well as infertile men with both known and unknown causes of infertility. The cohort was used to evaluate whether previous observed SP glycosylation changes with fertility were related to PSA. The developed assay has the potential to be further applied for different clinical questions, for example in prostate cancer studies, as well as to be extended to study the glycosylation of PSA from different body fluids (e.g. urine and serum).

2. Materials and methods

2.1. Materials

2.1.1. Chemicals and standards (see Supplementary Information S-1.1)

.

2.1.2. Clinical samples

SP samples were collected from infertile men (24–49 years old) who participated in an intrauterine insemination procedure with their partners at the 2nd Clinic of Gynaecology and Obstetrics, Wrocław Medical University (N = 85). The control group consisted of SP samples from fertile volunteers (N = 17), who had fathered a child within recent years. Semen samples were obtained through masturbation, after 2–3 days of sexual abstinence, and were liquefied for 1 h at 37 °C. Standard semen examination (volume, pH, morphology, sperm concentration, motility and viability) was performed for all individuals according to World Health Organization (WHO) directives [24] (Table 1). Based on this, samples from infertile men were subdivided into the following four groups: asthenozoospermic (A; total sperm motility < 40%), oligozoospermic (O; sperm count < 15×10^6/mL), oligoasthenozoospermic (OA; sperm count < 15×10^6/mL and total sperm motility < 40%) and normozoospermic (N; semen parameters within WHO normal range). After the standard semen examination, spermatozoa were gently centrifuged (400×*g*, 10 min at RT). The obtained SP was aliquoted and stored at −80 °C. Male infertility was diagnosed after at least one year of unprotected intercourse without achieving pregnancy. Couples were excluded from the study when female factors played a role in the infertility. These were defined as an abnormal structure of the reproductive tract (examined by ultrasound), abnormal ovulation and the occurrence of endometriosis. All participants provided written informed consent and the study was approved by Wrocław Medical University Bioethics Council (approval number KB-451/2016). For assessment of the intra- and interday variation of the assay, a pool of all individual samples was used (TPool). As positive controls for the cohort analysis, five pools of individual samples per group (N, O, A, OA and C) were used (GPools), which were each included randomly throughout the cohort 7 to 10 times. The concentration of PSA in the TPool of SP was determined via standard addition (Supplementary Information S-1.2 and 1.3).

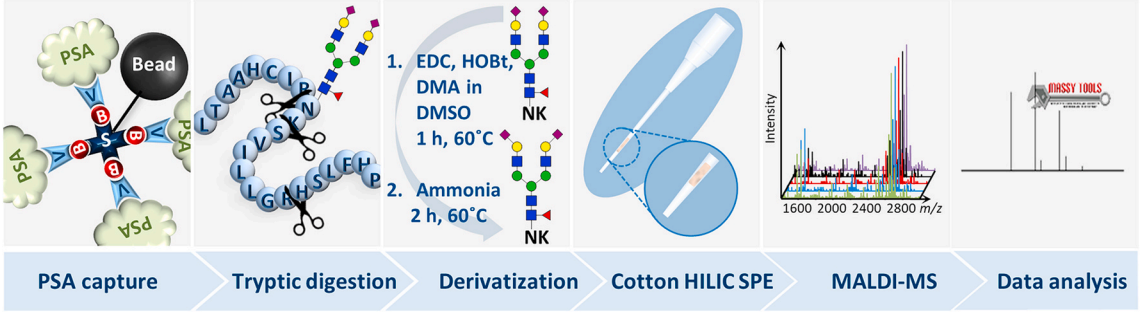

Fig. 1. High-throughput PSA glycopeptide analysis workflow. PSA was enriched from SP by immunoaffinity capturing (overnight; ON). After capturing, PSA was digested by trypsin (ON), resulting in PSA glycopeptides with two amino acids (Asn-Lys; $N_{69}K$). A two-step sialic acid linkage-specific derivatization (3 h) was performed followed by cotton hydrophilic interaction liquid chromatography (HILIC)-solid phase extraction (SPE) clean-up (8 min per 12 samples). Finally, samples were measured by MALDI-MS (30 s per sample). The complete procedure takes 2.5 days and four 96-well plates can be processed in parallel. Data analysis was performed using MassyTools and R language.

Table 1
Characteristics of the clinical samples.

Group[a]		Age		Sperm count		Sperm motility	
		Median	Range	Median [x 10^6/mL]	Range [x 10^6/mL]	Median [%]	Range [%]
C	(N = 17)	32	26–39	57.9	31.2–145.0	50	35–71
A	(N = 20)	34	29–47	35.7	19.0–94.7	24	4–30
O	(N = 20)	32	27–40	8.1	3.0–11.2	47	33–67
OA	(N = 20)	34	24–49	6.0	0.3–10.8	19	1–29
N	(N = 25)	34	28–40	61.9	26.0–109.7	52	33–67

[a] N: normozoospermic, O: oligozoospermic, A: asthenozoospermic, OA: oligoasthenozoospermic, C: fertile controls.

2.2. Anti-PSA beads

To prepare the *anti*-PSA beads, 6.4 mg biotinylated VHH *anti*-PSA antibodies (bVHH-aPSA) was added to 3500 μL drained high-capacity streptavidin agarose resins and the mixture was incubated overnight (ON) at 4 °C on a tube roller. The beads were spun down by centrifugation (100×*g*, 2 min), the supernatant was removed and beads were washed twice with 5 mL freshly prepared PBS. Next, beads were re-suspended in 15 mL of 100 mM formic acid (FA, freshly prepared) and shaken for 5 min. Again, beads were spun down, the supernatant was removed and beads were washed with 15 mL PBS to restore the pH. Beads were stored as 50% suspension in PBS containing 0.02% NaN_3 at 4 °C. Coupling efficiency was determined to be 88% by means of SDS-PAGE (Supplementary Information Figure S-1; Supplementary Information S-1.4).

2.3. PSA capturing

The optimal volume of SP for PSA capturing was determined in a 96-well filter plate format. For this purpose, 3, 5, 10 or 20 μL TPool SP was incubated with 4 μL of 50% beads suspension and 20 μL PBS on the filter. For all conditions, the plate was sealed and incubated ON at 4 °C on a plate shaker (1300 rpm, Heidolph Tiramax 100 platform shaker, Heidolph, Schwabach, Germany). Afterwards, the liquid was removed from the beads using a vacuum manifold followed by washes with 600 μL PBS and two times with 600 μL of 50 mM ammonium bicarbonate (ABC). Captured PSA was eluted into a low protein binding flat bottom plate (polypropylene plate, Greiner Bio-One, Kremsmünster, Austria) by centrifugation (100×*g*, 2 min), after incubation (5 min, with agitation) with 200 μL of 100 mM FA. The samples were dried by vacuum concentration at 45 °C for 2 h. The same procedure was performed to find the optimal volume of beads. Here, 4, 6, 8 or 10 μL 50% bead suspension was added to 10 μL TPool SP and 20 μL PBS. In all cases, capturing efficiency was evaluated by SDS-PAGE (Supplementary Information S-1.5). All experiments were performed in duplicate.

The final protocol for the high-throughput capturing of PSA from SP used 10 μL SP in combination with 20 μL PBS and 6 μL 50% aPSA bead suspension. After capturing, the PSA samples were reduced and alkylated, followed by a tryptic digestion as described before [15] (Supplementary Information S-1.6).

2.4. Sialic acid derivatization

Two previously described types of SA derivatization were initially applied on the PSA glycopeptide samples, namely dimethylamine amidation of α2,6-linked SAs in combination with ammonia amidation of α2,3-linked SAs (DA) [20], and ethyl esterification of α2,6-linked SAs in combination with ammonia amidation of α2,3-linked SAs (EEA) [18]. To minimize the degree of byproducts formed and to retain maximum linkage-specificity, a set of optimization experiments was performed (Supplementary Information Table S-1 and 2). All conditions were tested in either 3 or 4 replicates. For the DA strategy [20], variations were evaluated for the first step of the reaction regarding the concentration of the dimethylamine (100, 150, 200 and 250 mM) as well as the reaction temperature (37 and 60 °C) and time (0.25, 0.5 and 1 h). For the EEA strategy the volume of ammonium hydroxide (4, 6 and 8 μL of a 28% solution) used in the second step of the reaction was evaluated, as well as the overall reaction temperature (37, 45 and 60 °C). The final protocol was based on the DA strategy [20]. Briefly, 2.4 μL of the tryptic PSA digest was incubated together with 20 μL dimethylamidation reagent (250 mM 1-ethyl-3-(3-(dimethylamino)propyl)-carbodiimide hydrochloride (EDC), 500 mM 1-hydroxybenzotriazole hydrate (HOBt) and 250 mM dimethylamine in DMSO) at 60 °C for 1 h in a 96-well plate. Subsequently, 8 μL of 28% ammonium hydroxide solution was added and the samples were incubated for another 2 h at 60 °C. Immediately after SA derivatization, the PSA glycopeptides were enriched from the reaction mixture using cotton HILIC SPE, as described previously [25] (Supplementary Information S-1.7).

2.5. MALDI-FTICR-MS

To prepare the samples for MALDI-Fourier-transform ion cyclotron resonance (FTICR)-MS analysis, 3 μL of the HILIC-SPE eluates were spotted on a MTP Anchorchip 800/384 MALDI target (Bruker Daltonics, Bremen, Germany), together with 1 μL matrix (5 mg/mL super-DHB in 50% acetonitrile containing 1 mM sodium hydroxide). The spots were left to dry at RT. MALDI-FTICR-MS analysis of the clinical cohort sample was performed on a 15 T solariX XR FTICR MS (Bruker Daltonics) equipped with a CombiSource and a ParaCell (Bruker Daltonics) under ftmsControl (version 2.1.0). All spectra were generated from 200 laser shots with a laser frequency of 500 Hz. Each spectrum was acquired at *m/z* 1011 to 5000 with 1 M data points (i.e., transient length of 2.307 s) and consisted of ten acquired scans. The excitation power and sweep step time were at 57% and 15 μs, respectively [26].

2.6. Repeatability assessment

To demonstrate the robustness of the method, the complete protocol including PSA capturing, digestion, derivatization, cleanup and MS analysis was performed on three separate days, with 12 replicates of the TPool each day. All samples spotted on the MALDI target were measured with MALDI-time-of-flight (TOF)-MS (Supplementary Information S-1.8) first, followed by MALDI-FTICR-MS.

2.7. CE-ESI-MS/MS

CE-ESI-MS(/MS) [15] was used to confirm the PSA glycoforms identified by MALDI-FTICR-MS in the SP PSA standard and to compare glycosylation profiles of the SP PSA standard to the ones obtained by MALDI-MS (Supplementary Information S-1.9).

2.8. Data processing

MALDI -MS spectra were manually screened for glycopeptides based on accurate mass, using DataAnalysis 5.0 (Build 203.2.3586, for FTICR-MS data) and flexAnalysis 3.4 (Build 76, for TOF-MS data). Spectrum calibration, targeted data extraction and analyte and spectra quality control were performed with MassyTools (version 1.0.0). The quality of

analytes was evaluated per spectrum and individual glycoforms were included for further data analysis when present in over half of all samples. An analyte was considered present in one sample when it had a signal-to-noise (S/N) ratio above 9, an isotopic pattern quality score below 0.5 and the ppm error between −5 and 5 (FTICR-MS) or between −20 and 20 (TOF-MS). Spectra curation was performed based on the total intensity of all analytes in one spectrum and the number of analytes identified in the spectrum. Spectra were excluded if the total intensity of all analytes was below the mean minus 3 times standard deviation (SD) and/or the number of analytes identified was lower than 31 (half of the highest number of analytes detected in the individual spectra). Finally, the absolute areas of the included analytes were normalized to the summed absolute area of all analytes in one spectrum (total area normalization). Derived traits were calculated based on specific glycosylation features, including the degree of fucosylation, differently linked sialyation, (sialylated) LacdiNAc on the antennae and *N*-glycan types (Table 2; Supplementary Information Table S–3).

Table 2
Description of derived traits.

Derived Trait	Depiction[a]	Description
Fucosylation	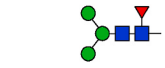	Fucosylation of all complex-type glycans
α2,3-sialylation	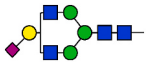	Sialylation, α2,3-linked to galactose, of di-antennary complex-type glycans
α2,6-sialylation	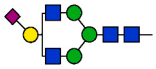	Sialylation, α2,6-linked to galactose, of di-antennary complex-type glycans
Ratio between α2,3- and α2,6-sialylation	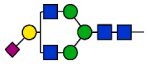 divided by	The ratio between α2,3-linked galactose-linked sialylation and α2,6-linked galactose-linked sialylation, of di-antennary complex-type glycans
Total α2,6-sialylation	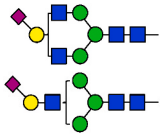 and	α2,6-linked sialylation of all complex-type glycans
LacdiNAc	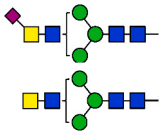	LacdiNAc motives on di-antennary complex-type glycans
Sialylated LacdiNAc	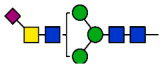	Sialylated (α2,6-linked) LacdiNAc motives on di-antennary complex-type glycans
Mono-antennary	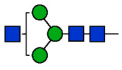	Fraction of mono-antennary glycans
High mannose- and hybrid-type	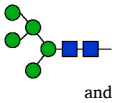 and 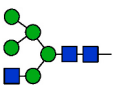	Fraction of high mannose- and hybrid-type glycans

[a] The depictions of the derived traits are the minimally required glycan compositions to be involved in a trait. For detailed on trait calculations, see Table S-3 in Supplementary Information.

2.9. Statistical analysis

Further data analysis of the clinical samples was carried out using R (version 3.4.3, R Foundation for Statistical Computing) together with RStudio (version February 1, 1335). Strip charts of the normalized glycopeptide values as well as the derived traits of individual samples and pooled samples were plotted per 96-well plate to reveal potential batch effects (no batch effects observed). Biological outliers were defined as a relative intensity that exceeded the range of the mean ± 5 SD per sample group (no biological outliers observed). The data was visualized by principle component analysis (PCA; R, pcaMethods [27]) and box plots (R, boxplot) of the five biological groups. Statistical differences among the five sample groups were analyzed using the Kruskal Wallis test (R, kruskal. test). The reported cut-off values for statistical testing were corrected by Benjamini-Hochberg Correction.

3. Results and discussion

Here, a method was developed for the high-throughput profiling of SP PSA glycosylation using MALDI-MS. The analysis was performed at the glycopeptide level, providing protein-specific information, and enabled the discrimination between α2,3- and α2,6-sialylated isomers with MS via linkage-specific derivatization.

3.1. PSA capturing from SP

The concentration PSA in the TPool of SP was determined to be approx. 0.8 μg/μL (Supplementary Information Figure S-2). The volumes of beads and SP used for the filter-plate-based capturing were optimized by first increasing the volume of SP while keeping the amount of beads constant (2 μL). A plateau was reached using 10 μL of SP and the recovery was further improved by increasing the volume of aPSA beads to 3 μL in the final protocol (Supplementary Information Figure S-3). This approach resulted in a capturing efficiency of about 21% ± 2%. The glycosylation profiles obtained using the different capturing conditions were highly comparable, indicating no glycoform-specific biases in the procedure. This is in agreement with a previous study which used the same capturing antibody for urine samples [15].

3.2. Linkage-specific SA derivatization at the glycopeptide level

After the tryptic digestion of PSA, the resulting glycopeptides carry a two-amino acid peptide moiety, namely, Asn-Lys. To both stabilize the sialylated species and allow the differentiation between SA linkage isomers in MS, two derivatization strategies were evaluated [18,23]. These strategies were previously established for the modification of released *N*-glycans on tissue (DA) [23] or in solution (EEA) [18]. However, SA derivatization at the glycopeptide level comes with additional challenges, as the peptide moieties carry groups that are prone to react with the added reagents in a variable manner [20,21]. For example, peptide carboxylic acids may react with the added nucleophile to form an ester or amide. Alternatively, internal reactions may be induced, resulting in lactam or lactone formation.

The EEA approach resulted for the most abundant PSA glycopeptide [H5N4F1$S_{2,6}$2]-Asn-Lys (H: hexose, N: *N*-acetylhexosamine, F: fucose, S: sialic acid) in two ethyl esters on the α2,6-SAs. Furthermore, the most abundant product (88.3% ± 4.9% SD) showed the loss of water from the peptide portion (2672.020 Da). However, the interpretation of the spectra and integration of the peaks was complicated by the formation of byproducts. These included ethyl esterification of the C-terminus (2718.062 Da; 2.0% ± 0.3 SD) instead of the loss of water and an unidentified byproduct (+171.112 Da) for each glycopeptide (9.7% ± 4.7% SD). Moreover, the EEA procedure resulted in under-amidation of α2,3-SAs, exemplified by the lactone on the α2,3-SA of the glycopeptide [H5N4F1$S_{2,3}$1$S_{2,6}$1]-Asn-Lys (2625.978 Da).

The optimized DA approach resulted for the PSA glycopeptides in

considerably less byproducts. The most abundant glycoform ($H5N4F1S_{2,6}2$) was two times dimethylamine amidated at the α2,6-SAs, while the main reaction on the Asn-Lys peptide (93.9% ± 1.7% SD) was the loss of water (2670.052 Da; Fig. 2; Supplementary Information Figure S-4). The remaining 6.1% (±1.7% SD) was C-terminally amidated with dimethylamine (2715.110 Da; Fig. 2; Supplementary Information Figure S-4). The minor amount of byproduct had limited effect on the data interpretation as the S/N of the resulting peaks was below 9 for all glycoforms except the most abundant one ($H5N4F1S_{2,6}2$). Hence, the DA approach was used for further method evaluation.

3.3. Method robustness

Intra- and interday repeatability of the complete workflow, including bead-based PSA isolation from SP, tryptic digestion, SA derivatization by DA, HILIC-SPE cleanup, sample spotting on a MALDI target and MALDI-FTICR-MS or MALDI-TOF-MS analysis, were evaluated using the TPool. In total, 44 glycoforms, including SA linkage isomers, were detected by MALDI-FTICR-MS (Fig. 3). The obtained glycosylation profiles were highly comparable over different days, showing a relative standard deviation (RSD) of 11.0%, 8.9%, 8.9% (intraday 1, 2, 3) and 11.2% (interday) for the main glycoform ($H5N4F1S_{2,6}2$; Fig. 3) and a median RSD of the 20 most abundant glycoforms of 10.4%, 10.0%, 13.9% and 13.5%, respectively. By using MALDI-TOF-MS, 22 glycoforms could be reliably quantified in the same sample (Supplementary Information Figure S-6). The higher number of glycoforms in the MALDI-FTICR-MS analyses was attributed to the higher resolution and sensitivity of the FTICR instrument as compared to the TOF-MS [28,29]. Comparing the intra- and interday repeatability of the two MS instruments, the FTICR-MS slightly outperformed the TOF-MS (Fig. 3; Supplementary Information Figure S-6). Despite its inferior performance in resolving power and mass accuracy as compared to MALDI-FTICR-MS, MALDI-TOF-MS is a powerful method for the analysis of derivatized PSA glycopeptides due to its broad availability and ease of operation. In addition, less in-source decay was observed using the TOF instrument. This shows that robust results can be obtained with the developed workflow using different MALDI-MS instruments.

3.4. Seminal PSA glycosylation

The optimized workflow with MALDI-FTICR-MS detection was applied to the clinical samples, resulting in 44 glycoforms that could be reliably quantified for glycosylation site Asn_{69} in all samples (Fig. 3; Supplementary Information Table S–4). The previously reported glycosylation site of the PSA isoform $D_{102}\rightarrow N_{102}$ were undetectable using the current MALDI-MS methods, as the expected larger tryptic glycopeptides would be out of reach in the used *m/z* range [10]. However, in the CE-ESI-MS analysis of the TPool sample, this site was also not found. SP PSA glycosylation revealed to be highly heterogeneous, with a high level of fucosylation (ranging from 49.1% to 77.8% in fertile controls) and sialylation (95.3%–98.8%) on mono- and di-antennary complex-type glycans. In addition, both hybrid-type and high mannose-type glycans were observed, ranging from 1.9% to 3.8% and 0.2%–1.9%, respectively. Interestingly, these results are similar to what was previously

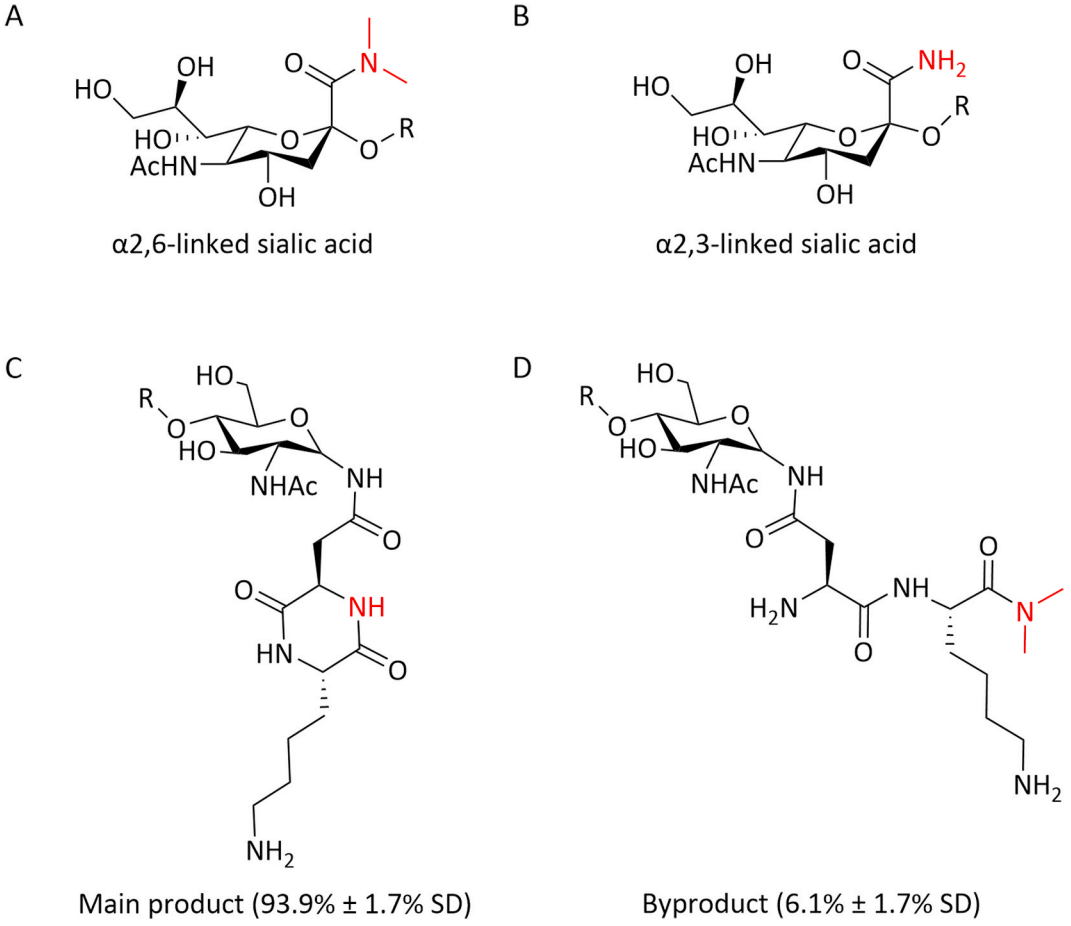

Fig. 2. Linkage-specific SA derivatization at the glycopeptide level. (A) Dimethylamine amidated α2,6-linked SA. **(B)** Ammonia amidated α2,3-linked SA. **(C)** The main modification of the peptide moiety (Asn-Lys) involved the loss of water via lactam formation between the C-terminus and the N-terminus (six-ring; as shown) or the C-terminus and the lysine side chain (seven-ring; Supporting Information **Figure S-4**). **(D)** The minor byproduct resulted from dimethylamine amidation of the C-terminus. 'R' shown in molecular structures stands for the rest of the glycan moiety.

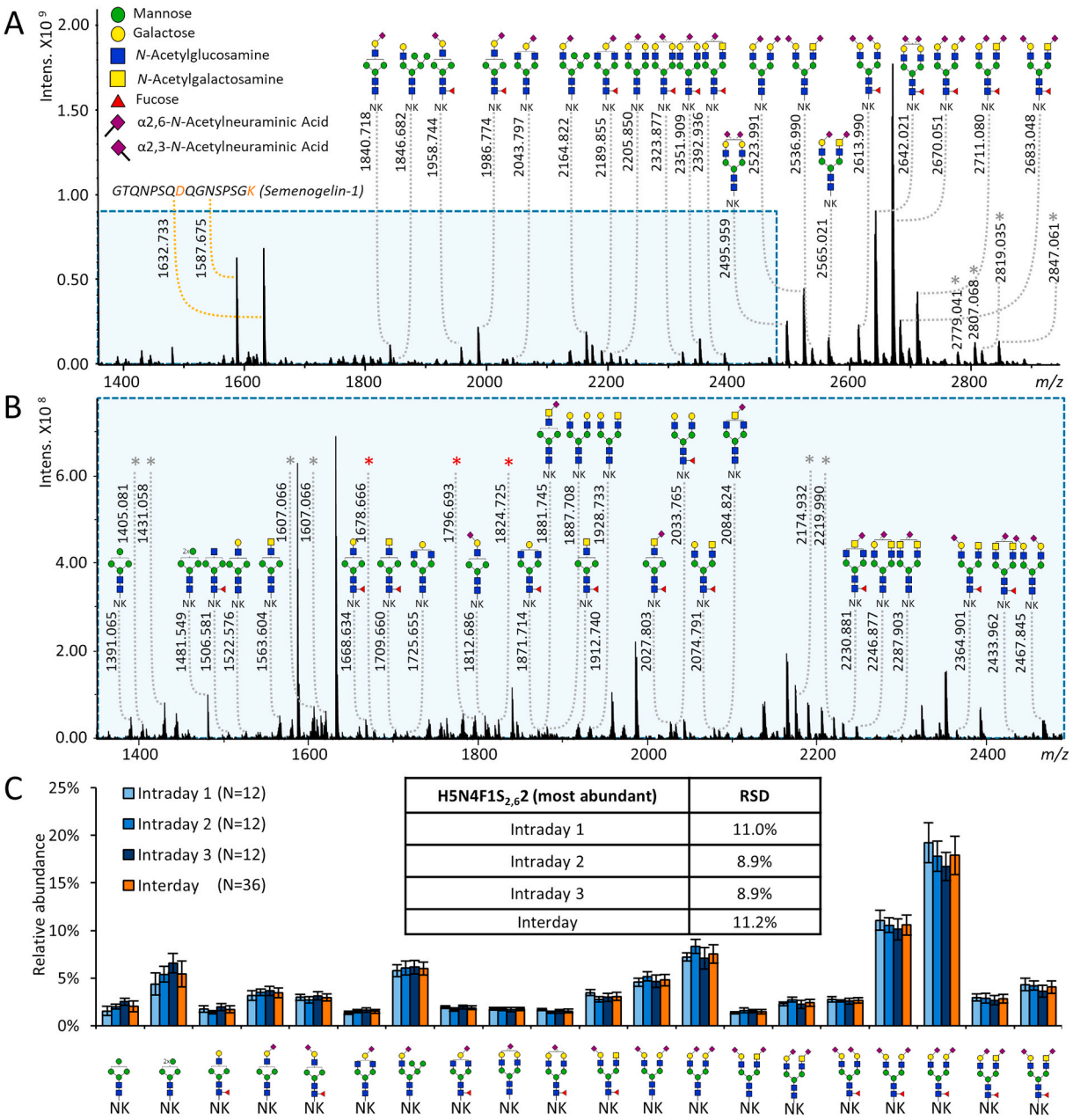

Fig. 3. Representative MALDI-FTICR-MS spectrum of SP PSA glycopeptides and their robust quantification. (A) Annotation of the 20 most abundant glycoforms in the TPool sample. **(B)** Zoom-in of the marked area in **(A)** with annotations of the 24 low abundant analytes. All annotated glycoforms were reliably quantified in all biological samples. The signals at *m/z* 1587.675 and 1632.733 were identified to be derived from the peptide GTQNPSQDQGNSPSGK from the seminal plasma protein semenogelin-1, carrying two different peptide modifications. Two times dimethylamidated, on both amino acid 'D' and the C-terminus were found at *m/z* 1587.675 and one time dimethylamidated with one water loss at *m/z* 1632.733. Peaks indicated with a grey asterisk are contaminants that could not be assigned to a (glyco)peptide. Peaks indicated with a red asterisk are insource decay products, which were also observed and assigned based on migration time using CE-ESI-MS. **(C)** Relative abundances of the 20 most abundant glycopeptides showing the intra- and interday repeatability of the method. Blue: intraday 1, 2 and 3, orange: interday. Error bars represent the standard deviation. The 24 lowest abundant glycopeptides can be found in **Figure S-5** (Supporting Information). H: hexose. N: *N*-acetylglucosamine. F: fucose. S: sialic acid. NK in spectrum annotation stands for peptide moiety of PSA glycodipeptides (Asn-Lys). (For interpretation of the references to color in this figure legend, the reader is referred to the Web version of this article.)

described for urinary PSA glycosylation in men with elevated PSA concentrations in serum, showing a fucosylation between 55% and 82% and a sialylation between 84% and 99% [15]. Additionally, tri- and tetra-antennary glycans were reported with high fucosylation and sialylation for serum PSA in men with elevated PSA levels [30]. With the current method, we were able to quantify the relative levels of α2,3- and α2,6-linked sialylation, showing that α2,6-sialylation was the most abundant linkage variant on SP PSA (76.1%–93.7%), which is in accordance with other studies on SP PSA [31] or PSA from different biofluids [32]. The profiles obtained for the PSA standard with the current MALDI-FTICR-MS method were comparable to the profiles obtained using an established CE-ESI-MS approach [31] (Supplementary Information Figure S-7; Table S–5). This indicates that the results obtained in the current study can be well compared to other studies into PSA glycosylation, performed by CE-ESI-MS [15]. The majority of all glycoforms detected by MALDI-FTICR-MS were confirmed by complementary CE-ESI-MS of the SP PSA standard.

Using CE-ESI-MS/MS, the PSA glycopeptides with glycan

compositions H4N5F1$S_{2,6}$1 and H4N5F1$S_{2,3}$1, were assigned to diantennary structures carrying a LacdiNAc motive on one of the antennae, via the detection of the diagnostic oxonium ion at *m/z* 407.166 ($[N2+proton]^+$; Supplementary Information Figure S-8). The absence of a signal at *m/z* 772.293 ($[N3H1+proton]^+$) indicated that no species were present carrying a bisecting GlcNAc. Furthermore, the LacdiNAc motive was found to carry exclusively α2,6-SAs as described previously [33,34]. The diagnostic oxonium ion of the sialylated LacdiNAc (*m/z* 698.261) was only found for the H4N5F1$S_{2,6}$1 isomer (first migrating analyte in the CE separation [15]; Supplementary Information Figure S-8). The LacNAc arm, on the other hand, can carry both types of SA linkages (*m/z* 657.235: $[H1N1S1+proton]^+$ was found for both H4N5S1 isomers; Supplementary Information Figure S-8).

3.5. PSA glycosylation and fertility

For the 44 glycoforms relatively quantified in the 102 individual samples, derived glycosylation traits were calculated. These traits summarized important glycosylation features of PSA [2–4], such as the levels of fucosylation, α2,3-sialylation, α2,6-sialylation and (sialylated) LacdiNAc antennae [30,35] on di-antennary glycans as well as the abundance of mono-antennary, hybrid- and high mannose-type glycans (Table 2; Supplementary Information Table S–3). By comparing the derived traits between the different biological groups (A, C, N, O, OA), no differences were observed between fertile and infertile men (Fig. 4; Supplementary Information Figure S-9; Table S-6 and 7). In addition, no glycosylation differences could be attributed to the different known causes of infertility (Fig. 4; Supplementary Information Figure S-9). Finally, no correlations were found between PSA glycosylation and age, sperm count or sperm motility in any of the groups (Supplementary Information Table S–8). The fact that the technical replicates of the GPool samples clustered together during the PCA analysis (Supplementary Information Figure S-9), while a large variation was observed in the PSA glycosylation of the individual samples, provided us with the confidence that the current method would have been able to pick-up relevant biological variations between the groups, if these would have been present. Total SP fucosylation and sialylation were previously reported as the main drivers behind the glycosylation effects found in infertility studies [2–4]. For example, *Sambucus nigra* agglutinin (SNA)-reactivity, indicating the presence of α2,6-SA, was reported to be lower in the SP of asthenozoospermic infertile men as compared to normozoospermic infertile and fertile men, while *N*-glycan β1, 6-branching as assessed by *Phaseolus vulgaris* leucoagglutinin (PHA-L)--reactivity was associated with a higher sperm count [3]. Furthermore, a MALDI-TOF-MS study of released *N*-glycans from total SP showed that highly fucosylated *N*-glycans were more abundant in asthenozoospermic, oligozoospermic and oligoasthenozoospermic infertile men as compared to normozoospermic infertile and fertile men [2]. Moreover, sialylation was found to be higher in normozoospermic infertile subjects as compared to asthenozoospermic. While the high level of fucosylation, that was associated with infertility, was previously suggested to be (partly) derived from PSA [4], we could not confirm this with the current cohort (Fig. 4). This suggests that the SP fucosylation is rather influenced by one or more of the other suggested SP proteins, like prostatic acid phosphatase or fibronectin 3. Moreover, while LacdiNAc and sialylated LacdiNAc signatures on serum PSA were previously associated with prostate cancer [30,35,36], no effects of this feature were found for infertility in the current study.

Of note, previous infertility studies assessing SP glycosylation focused on total SP [2–4] and to our knowledge, no reports were made on individual SP proteins. Furthermore, some studies only assessed the differences in SP glycosylation between pools of SP samples [2–4], which caused the biological differences between individuals to be lost, likely resulting in an overestimation of glycosylation effects in the population. Finally, the reported increase of highly branched [3] and multi-fucosylated *N*-glycans with infertility [2,3] is unlikely to be derived from SP PSA, as only mono- and di-antennary glycans with one fucose were found.

4. Conclusion

A novel, high-throughput SP PSA glycopeptide analysis workflow has been established using MALDI-FTICR-MS. The method shows an excellent repeatability over the analysis of more than 100 biological samples and was able to relatively quantify 44 glycoforms of PSA from SP. The implemented SA derivatization allows SA linkage discrimination by MS and results in minimal byproduct formation on the peptide portion of the PSA glycopeptides. Performing the analysis at glycopeptide level provides glycosylation site- and protein-specific information. The sample preparation is also compatible with MALDI-TOF-MS analysis, albeit with a lower number of glycoform identifications. This makes the method attractive for a broader range of glyco-analytical laboratories. Here, SP PSA was analyzed in the context of male infertility. We showed that the SP glycosylation changes previously associated with male infertility are likely not caused by SP PSA glycosylation. Our method is well applicable to profile the glycosylation of PSA from SP and may be applied in different disease contexts in the future, for example focusing on prostate cancer. Furthermore, the high-throughput analysis of PSA

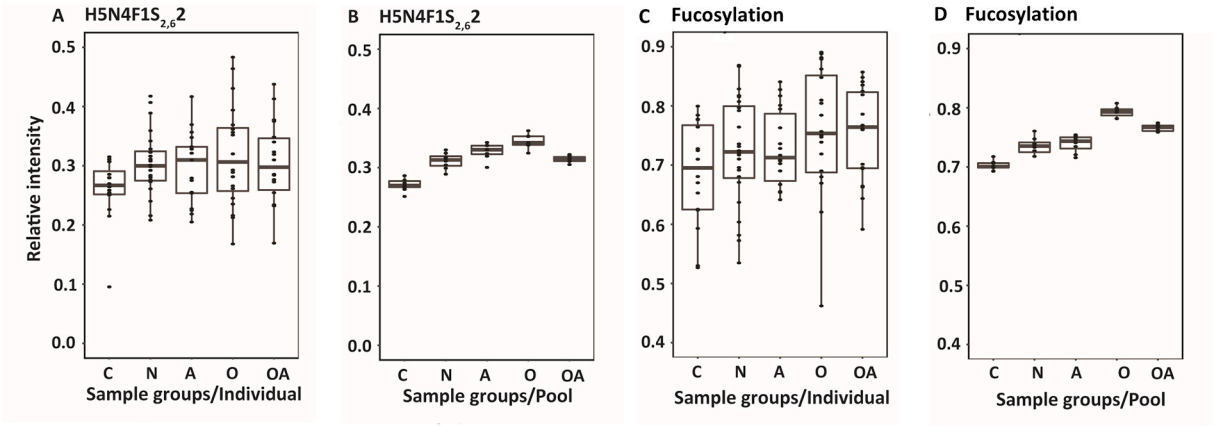

Fig. 4. Boxplot visualization of the clinical samples and the GPool replicates. (A) Boxplot showing the biological variation of the most abundant PSA glycoform [H5N4F1$S_{2,6}$2]-Asn-Lys per biological group. **(B)** Boxplot showing the technical variation of the most abundant PSA glycoform [H5N4F1$S_{2,6}$2]-Asn-Lys in the GPool samples per biological group. **(C)** Boxplot showing the biological variation of the PSA fucosylation per biological group. **(D)** Boxplot showing the technical variation of the PSA fucosylation in the GPool samples per biological group. N: normozoospermic, O: oligozoospermic, A: asthenozoospermic, OA: oligoasthenozoospermic, C: fertile controls.

glycopeptides may be combined with the capturing of PSA from different body fluids, such as urine or serum.

Author contributions

The manuscript was written through contributions of all authors. All authors have given approval to the final version of the manuscript. Contribution list shown as follow.

Wei Wang: Investigation, formal analysis, writing-original draft. Anna Kałuża: Investigation, resources, writing-original draft. Jan Nouta: Investigation. Simone Nicolardi: Investigation. Mirosława Ferens-Sieczkowska: Resources. Manfred Wuhrer: Conceptualization, supervision. Guinevere S.M. Lageveen-Kammeijer: Conceptualization, supervision, writing - review & editing. Noortje de Haan: Conceptualization, supervision, writing - review & editing.

Declaration of competing interest

The authors declare that they have no known competing financial interests or personal relationships that could have appeared to influence the work reported in this paper.

Acknowledgment

This work was supported by the China Scholarship Council.

Appendix A. Supplementary data

Supplementary data to this article can be found online at https://doi.org/10.1016/j.talanta.2020.121495.

References

[1] A. Varki, Biological roles of glycans, Glycobiology 27 (1) (2017) 3–49.
[2] A. Kałuża, A. Jarząb, A. Gamian, E.M. Kratz, M. Zimmer, M. Ferens-Sieczkowska, Preliminary MALDI-TOF-MS analysis of seminal plasma N-glycome of infertile men, Carbohydr. Res. 435 (2016) 19–25.
[3] E.M. Kratz, A. Kałuża, M. Zimmer, M. Ferens-Sieczkowska, The analysis of sialylation, N-glycan branching, and expression of O-glycans in seminal plasma of infertile men, Dis. Markers (2015) 941871.
[4] B. Olejnik, E.M. Kratz, M. Zimmer, M. Ferens-Sieczkowska, Glycoprotein fucosylation is increased in seminal plasma of subfertile men, Asian J. Androl. 17 (2) (2015) 274.
[5] H. Lilja, J. Oldbring, G. Rannevik, C. Laurell, Seminal vesicle-secreted proteins and their reactions during gelation and liquefaction of human semen, J. Clin. Invest. 80 (2) (1987) 281–285.
[6] M. Salam, Principles and Practice of Urology, JP Medical Ltd2013.
[7] G. De Angelis, H.G. Rittenhouse, S.D. Mikolajczyk, L.B. Shamel, A. Semjonow, Twenty years of PSA: from prostate antigen to tumor marker, Rev. Urol. 9 (3) (2007) 113.
[8] R.R. Drake, E.E. Jones, T.W. Powers, J.O. Nyalwidhe, Altered Glycosylation in Prostate Cancer, Advances in Cancer Research, Elsevier, 2015, pp. 345–382.
[9] E.A. Stura, B.H. Muller, M. Bossus, S. Michel, C. Jolivet-Reynaud, F. Ducancel, Crystal structure of human prostate-specific antigen in a sandwich antibody complex, J. Mol. Biol. 414 (4) (2011) 530–544.
[10] E. Song, Y. Hu, A. Hussein, C.-Y. Yu, H. Tang, Y. Mechref, Characterization of the glycosylation site of human PSA prompted by missense mutation using LC–MS/MS, J. Proteome Res. 14 (7) (2015) 2872–2883.
[11] N. Leymarie, P.J. Griffin, K. Jonscher, D. Kolarich, R. Orlando, M. McComb, J. Zaia, J. Aguilan, W.R. Alley, F. Altmann, Interlaboratory study on differential analysis of protein glycosylation by mass spectrometry: the ABRF glycoprotein research multi-institutional study 2012, Mol. Cell. Proteomics 12 (10) (2013) 2935–2951.
[12] K.Y. White, L. Rodemich, J.O. Nyalwidhe, M.A. Comunale, M.A. Clements, R. S. Lance, P.F. Schellhammer, A.S. Mehta, O.J. Semmes, R.R. Drake, Glycomic characterization of prostate-specific antigen and prostatic acid phosphatase in prostate cancer and benign disease seminal plasma fluids, J. Proteome Res. 8 (2) (2009) 620–630.
[13] S. Prakash, P.W. Robbins, Glycotyping of prostate specific antigen, Glycobiology 10 (2) (2000) 173–176.
[14] M. Tajiri, C. Ohyama, Y. Wada, Oligosaccharide profiles of the prostate specific antigen in free and complexed forms from the prostate cancer patient serum and in seminal plasma: a glycopeptide approach, Glycobiology 18 (1) (2007) 2–8.
[15] G.S.M. Kammeijer, J. Nouta, J. de la Rosette, T.M. de Reijke, M. Wuhrer, An in-depth glycosylation assay for urinary prostate-specific antigen, Anal. Chem. 90 (7) (2018) 4414–4421.
[16] J. Abrahams, N. Packer, M. Campbell, Relative quantitation of multi-antennary N-glycan classes: combining PGC-LC-ESI-MS with exoglycosidase digestion, Analyst 140 (16) (2015) 5444–5449.
[17] M. Pabst, F. Altmann, Glycan analysis by modern instrumental methods, Proteomics 11 (4) (2011) 631–643.
[18] K.R. Reiding, E. Lonardi, A.L.H. Ederveen, M. Wuhrer, Ethyl esterification for MALDI-MS analysis of protein glycosylation, Proteomics in Systems Biology, Springer2016, pp. 151-162.
[19] S.F. Wheeler, P. Domann, D.J. Harvey, Derivatization of sialic acids for stabilization in matrix-assisted laser desorption/ionization mass spectrometry and concomitant differentiation of α (2→ 3)-and α (2→ 6)-isomers, Rapid Commun. Mass Spectrom.: An International Journal Devoted to the Rapid Dissemination of Up-to-the-Minute Research in Mass Spectrometry 23 (2) (2009) 303–312.
[20] N. de Haan, K.R. Reiding, M. Haberger, D. Reusch, D. Falck, M. Wuhrer, Linkage-specific sialic acid derivatization for MALDI-TOF-MS profiling of IgG glycopeptides, Anal. Chem. 87 (16) (2015) 8284–8291.
[21] A.G. Gomes de Oliveira, R. Roy, C. Raymond, E.D. Bodnar, V.S. Tayi, M. Butler, Y. Durocher, H. Perreault, A systematic study of glycopeptide esterification for the semi-quantitative determination of sialylation in antibodies, Rapid Commun. Mass Spectrom. 29 (19) (2015) 1817–1826.
[22] S. Yang, W.W. Wu, R.-F. Shen, M. Bern, J. Cipollo, Identification of sialic acid linkages on intact glycopeptides via differential chemical modification using IntactGIG-HILIC, J. Am. Soc. Mass Spectrom. 29 (6) (2018) 1273–1283.
[23] S. Holst, B. Heijs, N. de Haan, R.J. van Zeijl, I.H. Briaire-de Bruijn, G.W. van Pelt, A. S. Mehta, P.M. Angel, W.E. Mesker, R.A. Tollenaar, Linkage-specific in situ sialic acid derivatization for N-glycan mass spectrometry imaging of formalin-fixed paraffin-embedded tissues, Anal. Chem. 88 (11) (2016) 5904–5913.
[24] World Health Organization, WHO Laboratory Manual for the Examination and Processing of Human Semen, fifth ed., 2010.
[25] M.H. Selman, M. Hemayatkar, A.M. Deelder, M. Wuhrer, Cotton HILIC SPE microtips for microscale purification and enrichment of glycans and glycopeptides, Anal. Chem. 83 (7) (2011) 2492–2499.
[26] G.C.M. Vreeker, S. Nicolardi, M.R. Bladergroen, C.J. van der Plas, W.E. Mesker, R. A.E.M. Tollenaar, Y.E.M. van der Burgt, M. Wuhrer, Automated plasma glycomics with linkage-specific sialic acid esterification and ultrahigh resolution MS, Anal. Chem. 90 (20) (2018) 11955–11961.
[27] W. Stacklies, H. Redestig, M. Scholz, D. Walther, J. Selbig, pcaMethods—a bioconductor package providing PCA methods for incomplete data, Bioinformatics 23 (9) (2007) 1164–1167.
[28] S. Nicolardi, B. Bogdanov, A. Deelder, M. Palmblad, Y. van der Burgt, Developments in FTICR-MS and its potential for body fluid signatures, Int. J. Mol. Sci. 16 (11) (2015) 27133–27144.
[29] S. Nicolardi, M. Palmblad, P.J. Hensbergen, R.A.E.M. Tollenaar, A.M. Deelder, Y.E. M. Burgt, Precision profiling and identification of human serum peptides using Fourier transform ion cyclotron resonance mass spectrometry, Rapid Commun. Mass Spectrom. 25 (23) (2011) 3457–3463.
[30] Y. Haga, M. Uemura, S. Baba, K. Inamura, K. Takeuchi, N. Nonomura, K. Ueda, Identification of multisialylated LacdiNAc structures as highly prostate cancer specific glycan signatures on PSA, Anal. Chem. 91 (3) (2019) 2247–2254.
[31] G.S.M. Kammeijer, B.C. Jansen, I. Kohler, A.A.M. Heemskerk, O.A. Mayboroda, P. J. Hensbergen, J. Schappler, M. Wuhrer, Sialic acid linkage differentiation of glycopeptides using capillary electrophoresis - electrospray ionization - mass spectrometry, Sci. Rep. 7 (1) (2017) 3733.
[32] R. Peracaula, G. Tabares, L. Royle, D.J. Harvey, R.A. Dwek, P.M. Rudd, R. de Llorens, Altered glycosylation pattern allows the distinction between prostate-specific antigen (PSA) from normal and tumor origins, Glycobiology 13 (6) (2003) 457–470.
[33] S. Lehoux, S. Groux-Degroote, A. Cazet, C.-M. Dhaenens, C.-A. Maurage, M.-L. Caillet-Boudin, P. Delannoy, M.-A. Krzewinski-Recchi, Transcriptional regulation of the human ST6GAL2 gene in cerebral cortex and neuronal cells, Glycoconj. J. 27 (1) (2010) 99–114.
[34] P.F. Rohfritsch, J.A. Joosten, M.-A. Krzewinski-Recchi, A. Harduin-Lepers, B. Laporte, S. Juliant, M. Cerutti, P. Delannoy, J.F. Vliegenthart, J.P. Kamerling, Probing the substrate specificity of four different sialyltransferases using synthetic β-D-Galp-(1→ 4)-β-D-GlcpNAc-(1→ 2)-α-D-Manp-(1→ O)(CH2) 7CH3 analogues: general activating effect of replacing N-acetylglucosamine by N-propionylglucosamine, Biochim. Biophys. Acta Gen. Subj. 1760 (4) (2006) 685–692.
[35] K. Hirano, A. Matsuda, T. Shirai, K. Furukawa, Expression of LacdiNAc groups on N-glycans among human tumors is complex, BioMed Res. Int. (2014) 981627.
[36] T. Inoue, T. Kaneko, S. Muramatsu, H. Kimura, T. Yoshino, T. Goto, A. Sawada, S. Akamatsu, T. Kobayashi, T. Yamasaki, T. Kaya, O. Ogawa, LacdiNAc-Glycosylated Prostate-specific Antigen Density Is a Potential Biomarker of Prostate Cancer, Clin Genitourin Cancer In press, 2019.